International Journal of Thermal Technologies
E-ISSN 2277 – 4114

Available at http://inpressco.com/category/ijtt/

Research Article

A contribution to a numerical characterization of the thermal transfers in a saw tooth solar collector

FOUAKEU NANFACK Gildas Armel†, TETANG FOKONE Abraham†‡*, EDOUN Marcel†*, KUITCHE Alexis†, ZEGHMATI Belkacem‡

†Laboratory of Energetics and Thermal Applied process (LETA), ENSAI, The University of Ngaoundere, B.o. 455, ENSAI-Ngaoundere, Cameroon
‡Laboratoire de Mathématique et de Physique (LA.M.P.S), Université de Perpignan via Domitia, 66860, Perpignan, France

Received 01 July 2019, Accepted 01 Sept 2019, Available online 02 Sept 2019, **Vol.9, No.3 (Sept 2019)**

Abstract

In this study, we have developed and modeled a saw tooth solar collector. It is a solar collector with single pass between the transparent cover and the absorber fixed on the insulator. The cover is double glasses with the plane upper glass and the lower glass in the shape from saw teeth. The absorber is also in the shape of saw tooth. After having chosen the mathematical models describing the thermal behavior of the prototype, the equations governing the transfers in the solar collector were based on the analogy between heat transfer and electric transfer. The algebraic systems of equations deduced from a discretization of these equations by an implicit method to finite differences are solved by Gauss algorithm. The theoretical characterization was compared with that experimental particularly for the collector outlet temperature and the absorber temperature. The analysis of the temperature profiles showed that at midday sun for an air velocity of 0.3 m/s, the temperature of the air at collector outlet for a theoretical characterization reaches 79.19 °C whereas that of the practical characterization is only 77.7 °C thus guaranteeing a total output of 22.15 %, and 22 % respectively for the theoretical characterization and the experimental when characterization sunshine is maximum. The results obtained by the models compared, concerning, show that calculations resulting from this study result closer to those from the undertaken experiments.

Keywords: *Solar collector, convection coefficient, saw tooth, thermal transfer, numerical characterization.*

1. Introduction

Solar energy has been used for a long time to produce heat and, although the accumulated experience is considerable, this field has experienced with the current technological development, a significant renewal on the theoretical and experimental level (Benkhelifa, 1998). The exploitation of this solar energy will therefore create inventions which will make it possible to install thermal solar collectors. These are defined as devices which make it possible to transform the solar radiation that they receive into usable heat energy through a heat transfer fluid which can be water or air for most cases (Jannot, 2011). The production of this thermal energy from solar energy by the air plane collectors knows nowadays knows many applications for their innumerable economic and environmental interests such as the production of electricity and the heating of homes or sanitary water by the thermodynamic power plants stations, and the drying of the agro-alimentary products by means of driers. For that, high outputs are required from the collectors (Benkhelifa, 1998).

*Corresponding Author: ORCID ID 0000-0003-4160-1796
DOI: https://doi.org/10.14741/ijtt/v.9.3.1

However, various works encountered show that the efficiency of an air plane solar collector is around 25 % (Semmar, *et al,* 1998; Njomo, 1998). This performance can be optimized on the one hand, by increasing the convective transfer coefficients between the absorbing plate and the coolant and on the other hand, by reducing the thermal losses through the various components of the solar collector. This optimization rests on several techniques, among them, one quotes the judicious choice of the adequate forms and the design parameters (geometrical, thermo-physical and optical) such as, the thickness of the channel, the thickness of the fluid air gap, the length and width of the collector, the thickness of insulator (for a good insulation), choice of selective or non selective absorbent material, single and double glazed, with multiple glass covers, polycarbonate or plastic film… etc).

Moreover, the plane solar collectors using air as heat transfer fluid are multiple. Thus, we distinguish the collectors with permeable absorber (Hwang *et al.,* 1999), the collectors with variable geometry absorber (Gao, *et al,* 2000; El-Sebaii, *et al,* 2011; Karim and Hawlader, 2006) and the plane collectors absorber

(Njomo, 1998; Oudjedi, *et al,* 2008; Tetang, *et al,* 2018), which are for more the most part simple air-pass collectors. No matter with type of collector is used, the thermal performance are related to the various exchange coefficients.

To improve this convective exchange coefficient between the air and the absorber, the researchers propose on the one hand the increase in the number of passage of the coolant. Thus we distinguish the air plane collectors with double air passes (El-Sebaii, *et al,* 2007; Tetang, *et al,* 2018), triple passes (Beikircher *et al,* 2015), and multiple passes (Kareem *et al,* 2016). In addition, some propose to introduce baffles (or obstacles) into the airstream of the collector. For that, Ahmed-Zaïd *et al,* (2001) use baffles of curved delta shaped longitudinal and arched ogival longitudinal in their work. The climate being sunny and very hot in this area, their results show that the exit temperatures of their air plane collector with obstacles can reach the value of 100°C at noon sun. In the same way, Moummi, *et al,* (2004), Youcef-Ali and Desmons (2006) and Bahria and Amirat (2013), presented a rather explicit analysis of the energy balance of an air plane solar collector fitted with rows of thin obstacles. The results obtained show the importance of using baffles for the improvement of the performance of the solar thermal collector. Also, the other shapes of baffles such as ogival (Abene, *et al,* 2004), trapezoidal (Labed, *et al,* 2009), and cylindrical base (Aouès, *et al,* 2011) were highlighted with satisfaction. Generally, these authors showed that the heat transfer, fluid outlet temperature and the collector are significantly improved.

However, the various performances hitherto obtained, remain always weak, therefore can still be optimized. It is in this logic that Djimasra (2014) experimentally characterized a new type of solar collector called *"a saw tooth solar collector",* which was designed and built Energy and Thermal Laboratory of the National School of Agro-industrial Sciences of the University of Ngaoundere. It increased the heat exchange transferring surface of the collector by forming the absorber and the second pane of the saw tooth collector. The results showed that by thus increasing the surface of the absorber of the collector without increasing its bulk, better thermal performances of the collector is obtained. It will therefore be a question for us, using the mathematical tools, to numerically characterize the thermal performance of the said collector.

2. Description of the saw tooth solar collector

This solar collector consists of a double transparent glass cover, one of which is a conventional surface plane and the other saw tooth shaped groove at an angle of 90°, of a sheet metal absorber painted galvanized steel and a plywood box (figure 1).

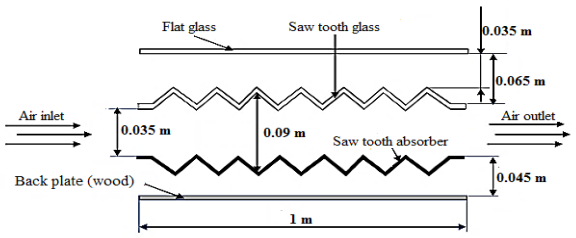

Fig.1 Saw tooth solar collector (Djimasra, 2014)

The geometric and thermo physical characteristics of the various elements and materials which constitute the collector are presented in Table 1.

Table 1 Characteristics of the various elements of the saw tooth solar collector

Components	Characteristics	Values
Box (thick wood 0.015 m)	Length (m)	1.030
	Width (m)	0.480
	Glass- back plate gap (m)	0.150
	Total thickness of the collector (m)	0.170
	Collector surface (m^2)	0.450
	Thermal conductivity (W/m°C)	0.200
	Thermal emissivity	0.100
Ordinary glass pane (Two glasses copanes)	Length (m)	1.000
	Width of the glass pane (m)	0.450
	Width of the saw tooth pane (m)	0.405
	Thickness (m)	0.004
	Thermal conductivity (W/m°C)	0.042
	Transparent cover transmittance	0.950
	Absorptance (dimensionless)	0.050
	Thermal emissivity	0.90
Absorber (galvanized steel painted black)	Length (m)	1.000
	Width (m)	0.405
	Thickness (m)	0.001
	Thermal conductivity (W/m°C)	46.000
	Absorptance (dimensionless)	0.95
	Thermal emissivity	0.96

3. Mathematical modeling

3.1 Principle of modeling

The principle of modeling consists of writing the energy balances on each element constituting the solar collector: the absorber, the cover glass, the insulator and the coolant, by using the slice modeling method.

This is a nodal method, also called the "step by step" method. It consists of cutting the collector into fictitious slices of identical length δx in the direction of the coolant flow heat and writing the balance sheets on each section. We will apply the electric analogy to heat transfer, the temperatures being assimilated to electric potentials, the density of the heat flow at intensities of the electric current, the heat transfer coefficients to electric resistances (Tetang, *et al,* 2018).

3.2 Simplifying assumptions

Within the framework of this work, the following simplifying assumptions are retained (Agbossou, *et al,* 2016; Tetang, *et al,* 2018):

- The physical properties of materials are supposed to be constant;
- Conduction in all materials perpendicular to the direction of the flow is neglected;
- The powers absorbed by the panes is negligible;
- Conduction through the absorber is neglected;
- The sky is comparable to a black body.

3.3 Assessment of energy

Figure 2 represents the components of the saw tooth collector and the different types of heat transfer involved.

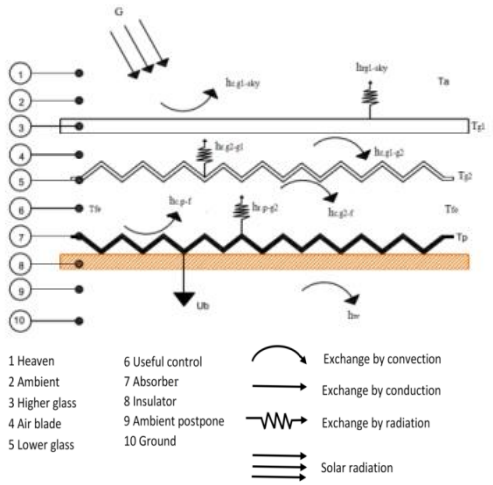

Fig. 2 Heat exchange in a section of a saw tooth solar collector

The equivalent electric diagram representing these various heat transfers is represented by figure 3.

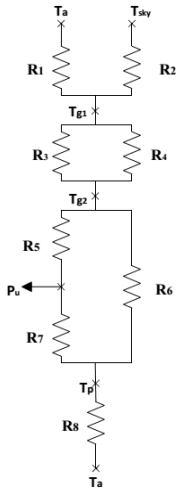

Fig. 3 Electrical model of the saw tooth solar collector

With $R_1 = \frac{1}{h_w}$; $R_2 = \frac{1}{h_{r.g1-sky}}$

$R_3 = \frac{1}{h_{c.g1-g2}}$; $R_4 = \frac{1}{h_{r.g2-g1}}$

$R_5 = \frac{1}{h_{c.g2-f}}$; $R_6 = \frac{1}{h_{r.p-g2}}$

$R_7 = \frac{1}{h_{c.p-f}}$; $R_8 = \frac{1}{U_b}$

Considering the previous simplifying assumptions, the various energy balance equations referred to in figure 3s' are generally written in the following form:

$$m_i * Cp_i\left(\frac{\partial T_i}{\partial t}\right) = \sum_{i,j=1}^{n} S.h_{xi,j}(T_j - T_i) + Pu_i \quad (1)$$

The establishment of thermal and mass report on all elements to the equations (2, 3, 4, 5).

- for plane cover glass (indice, g1)

$$\frac{m_{g1}*C_{pg1}}{s}\frac{\partial T_{g1}}{\partial t} = G\alpha_{g1} - h_{r.g1-sky}(T_{g1} - T_{sky}) - h_{r.g2-g1}(T_{g2} - T_{g1}) - h_w(T_{g1} - T_a) + h_{c.g1-g2}(T_{g1} - T_{g2}) \quad (2)$$

- for the saw tooth glass (indice, g2)

$$\frac{m_{g2}*C_{pg2}}{s}\frac{\partial T_{g2}}{\partial t} = G\alpha_{g2}\tau_{g1} - h_{r.g2-g1}(T_{g2} - T_{g1}) - h_{r.p-g2}(T_p - T_{g2}) + h_{c.g2-f}(T_{g2} - T_f) + h_{c.g1-g2}(T_{g2} - T_{g1}) \quad (3)$$

- For the absorber (index, p)

$$\frac{m_p*C_{pp}}{s}\frac{\partial T_p}{\partial t} = G\alpha_p\tau_{g1}\tau_{g2} - Zh_{c.p-f}(T_p - T_f) - h_{r.p-g2}(T_p - T_{g2}) - U_b(T_p - T_f) \quad (4)$$

Z being the ratio of the actual area of the absorber and the normal surface of solar radiation (Kabeel and Mecarik, 1998).

- Thermal balance of the useful coolant (indice, f)

$$\rho_f e_f c_{pf}\frac{dT_f}{dt} + \frac{\dot{m}_f C_{pf}}{l}\frac{dT_f}{dx} = h_{c.g2-f}(T_{g2} - T_f) - h_{c.p-f}(T_p - T_f) \quad (5)$$

In practice, the variations in the enthalpy time of the collector components are weak, i.e. the terms $m * C_p \frac{\partial T}{\partial t}$ can be neglected (Njomo, 1998).

3.4 Resolution method

Equations 2 to 5 were solved by using a semi-empirical method. The latter consists of expressing the temperatures T_a, T_p and T_f according to the other parameters whose values were experimentally determined.

3.5 Theoretical characterization of the solar irradiation and the ambient temperature

3.5.1 Theoretical characterization of the solar irradiation

Oudjedi, *et al,* (2008) proposes to calculate the total solar flows, direct and diffuse, incident on a horizontal level and at any moment as follows:

- The direct solar radiation is given by the following expression:

$$S = I.sin(h) \quad (6)$$

- The diffuse solar radiation from the sky is given by the following expression:

$$D = I_0\, sin(h)\left[0{,}271 - 0{,}2939 * a * exp\left(\frac{-b}{sin(h)}\right)\right] \quad (7)$$

- The global solar radiation incident on a horizontal level is expressed by:

$$G = D + S \quad (8)$$

With, I_0 which is the extraterrestrial radiation, given by the following formula:

$$I_0 = 1367 * [1 + 0{,}034 * cos(0{,}986 * j - 2)] \quad (9)$$

I is the direct solar radiation parallel to the solar ray given by the formula:

$$I = I_0 * a * exp\left(\frac{-b}{sin(h)}\right) \quad (10)$$

Oudjedi, *et al,* (2008) used cloud coefficients of disorder while taking a = 0.88 and b = 0.26. h indicates the height of the sun proposed by Jannot (2011).

3.5.2 Theoretical characterization of the ambient temperature

Tetang, *et al,* (2018) are modeling the ambient temperature by the following expression:

$$T_a = T_1 + T_2 * cos\left(\frac{\pi}{12} * (14 - t)\right) \quad (11)$$

$$T_1 = \frac{T_{a.max} + T_{a.min}}{2} \quad (12)$$

$$T_2 = \frac{T_{a.max} - T_{a.min}}{2} \quad (13)$$

With T_{max} and T_{min} ambient temperatures maximum and minimal of the day.

4. Results and discussion

This part is devoted to the presentation of the principal results of the study. Firstly, we will have the theoretical results of the characterization of the solar irradiation of the month when the test are carried out (April) and secondly, we will highlight the results of the thermal performance test.

4.1. Solar irradiation

Figure 4 presents the evolution of the calculated and measured irradiation thus putting forward the shift between the calculated and the measured values.

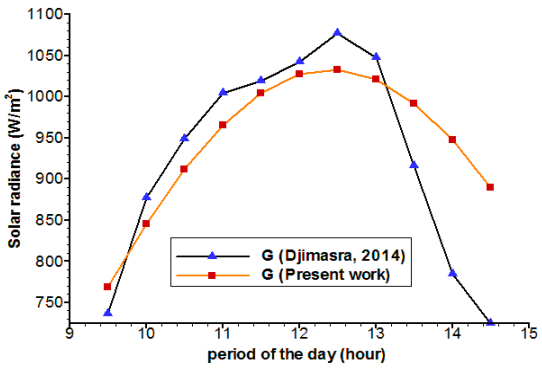

Fig. 4 Evolution of calculated and measured radiance

It arises from figure 4 that the two curves present the shape parabolic. This shows the increase and the decrease of sunshine during the day. By taking the theoretical curve like reference, we notice that the experimental curve presents irregularities in its daily progression because of the cloudy days running the sky corroborating with the work of Bahri and Amirat (2013). Solar flow evolves up to 1076.4 W/m² for the experimental characterization and 1032.6 W/m² for the theoretical. These values of solar flow prove the sufficiency of the sunshine for the solar collector performance since standard ASHRAE (American Society of Heating, Refrigerating and standard Air-Conditioning Engineers) requires that, for efficient tests of solar collectors, the solar radiation must be above 630 W/m² (Labed *et al,* 2013).

4.2. Profile of temperature

The curves relating to the evolution of the temperature of the absorber and that of air inlet and the air outlet the collector for the two studies are represented respectively on figures 5 and 6. It is noted that the experimental results coincide well with the results of analytical simulation, in the same way we observe at solar midday a considerable variation in temperature between the entry and the exit which is according to sunshine. This average gap is about 50.8°C for the experimental characterization and 53.8°C for the theoretical characterization.

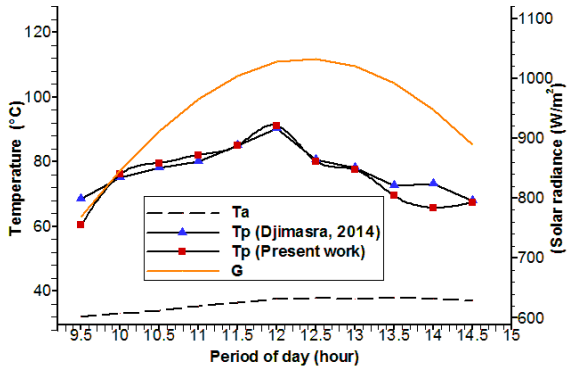

Fig.5 Evolution of the irradiance and the air temperature input/output of the absorber

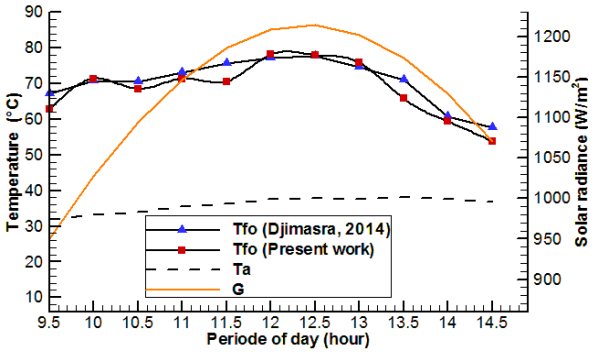

Fig.6 Evolution of the irradiance and the temperature of the air input/output of the collector

However, the temperature of exit of the collector is recorded with a maximum of 80.19°C with 12h (Standard time) near to the experimental study These results are in agreement with those of El-Sebaii, *et al,* (2011) which show the convergence of the two studies (experimental simulation and theoretical simulation).

4.3. Absorbed power

Figure 7 illustrates the time evolution of the absorbed power of the collector for the day of April 2014. From the analysis of these curves, the absorbed power increases and decreases with the sunshine. The examination of the curves below show that the values resulting from the theoretical study is very near to those recorded experimentally because, it varies in a similar way with an acceptable gap.

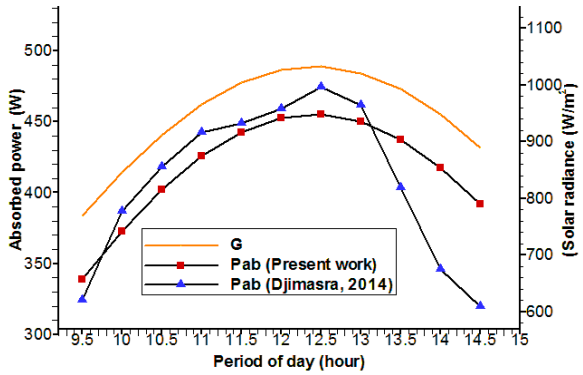

Fig.7 Evolution of irradiance and the absorbed power

One can conclude that, the results obtained by the compared models, concerning the absorbed power, show that the curve resulting from this study converges towards that resulting from the undertaken experiments.

4.4. Coefficient of exchange and a number of Nusselt

Figures 8 and 9 respectively present the evolution of the coefficient of heat exchange and the evolution of the radiance and the number of Nusselt of the saw tooth collector.

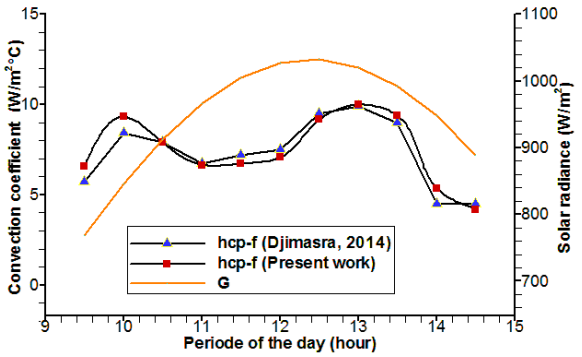

Fig.8 Evolution of the irradiance and the convection coefficient of air

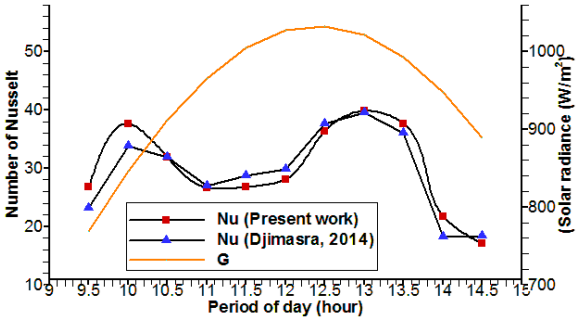

Fig.9 Evolution of the irradiance and the number of Nusselt

It comes out from the analysis of the curves that for experimental and theoretical characterizations, we can raise the highest coefficients of heat exchange (respectively 9.9 W/m²°C and 10.58 W/m²°C averages). These results show a bringing together of profiles of these two experimental and theoretical studies. It is noted that the experimental results coincide well with the results of the numerical simulation, in the same way one notes a minimal variation of the Number of Nusselt around 1 p.m.

4.5. Useful power

We present in figure 10 a comparison between the experimental results and those resulting from the theoretical analysis of evolution of the useful power according to the time of the saw tooth solar collector.

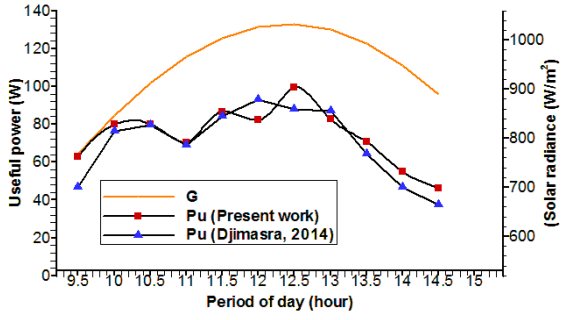

Fig.10 Evolution of irradiance and the useful power

It arises from the analysis of the curves that with 12h30 a.m for these two studies, one notices a considerable variation of 11.57 W. These results show a closeness of the profiles of these two experimental and theoretical studies.

4.6. Instantaneous global efficiency

Figure 11 shows the evolution of the instantaneous global efficiency according to time.

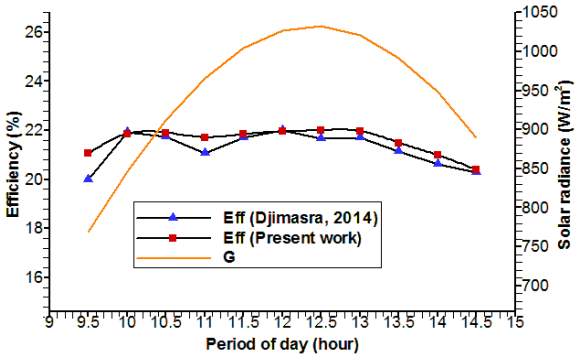

Fig.11 Evolution of radiance and the instantaneous global efficiency

From the analysis of the curves of this figure, one notes that the global efficiency is around 22% for the experimental study and 22.15% for the theoretical study at midday sun. One realizes that the two curves almost have the same profile similar to work of Bahri and Amirat (2013), which makes it possible to say that the selected model predicts better the output of our saw tooth collector.

Conclusion

The solar collector in teeth of saw was designed, produced and modeled at the Laboratory of Energetics and Thermics Applied of ENSAI of the University of Ngaoundéré. It is a double glazed solar collector. It is used to convert the radiant energy of the sun into thermal energy. Our work consisted in the theoretical study of an air solar collector with a simple pass between the cover glass and the absorber. To work out this work, we established the equations of heat balance translating the thermal behavior of our saw tooth collector then, we brought out the models able to facilitate these exercises which were coded in VBA (Visual Basic for Application). These equations enabled us to come out with the various profiles of irradiance, the temperature of the absorber, the outlet temperature, the number of Nusselt, the convection coefficient between the absorber-fluid and the thermal efficiency according to the time of the two studies. One observes from these curves that the agreements prove to be acceptable and the variations which exist are due on the one hand, to the errors of measurement, thermal inertia and the disturbances of the system (by cloudy passages). Thus, we can say that the models chosen with the assumptions used made it possible to better predict the thermal behavior of the saw tooth solar collector.

Nomenclature

$\dot{m}$ Mass flow of the air (kg/s)
m Mass of the material (kg)
ΔT Variation in temperature (°C)
S_c Surface collecting of the plane collector with air (m^2)
C_p Specific heat of the air (J/kg°C)
D_h Hydraulic diameter of the conduit of the fluid (m)
g Acceleration of gravity (m/s^2)
G Solar flow total receipt by the plane collector with air (W/m^2)
h Thermal coefficient of transfer ($W/m^2°C$)
Hr Relative humidity (%)
L Length characteristic of the collector (m)
P_v Pressure partial of water vapor in the air (mHg)
P_u Flow exchanged between the absorber and the air (W)
Q_v Voluminal flow of the air (m^3/s)
S Section of entry and exit of air (m^2)
T Temperature (°C)
V Velocity of flow of the air (m/s)
R Thermal resistance ($m^2°C$ /W)

Nombres adimensionnels

Gr Number of Grashof
Nu Number of Nusselt
Pr Number of Prandtl
Ra Number of Rayleigh

Symboles grecs

η Efficiency of the collector (%)
α Absorption coefficient
β Thermal dilation coefficient of the air ($°C^{-1}$)
ε Emissivity
λ Thermal conductivity of the air (W/m°C)
μ Dynamic viscosity of the air (Pa.s)
ρ Density (kg/m3)
σ Constant of Stefan-Boltzmann ($W/m^2°C^4$)
τ Coefficient of transmission of the cover glass
N Numbers of Glazing
θ Angle of inclination of the collector
e Thickness of the mobile vein of air (m)
t Time (period of the day) (h)

Indices

fe input fluid
fo output fluid
ab Absorber
w Wind
a ambiant
p Plate Absorbing
r Radiation
c Convection
x Mode of transfer of heat (irradiation, conduction or convection)
e Entry
f Fluid
s Exit
u Useful
g1 Plane cover glass
g2 Cover glass in saw tooth

References

A. Abene, V. Dubois, M. L. Ray and A. Ouagued, (2004), Study of a solar air flat plate collector: use of obstacles and application for the drying of grape. *Journal of Food Engineering*, Vol. 65, pp. 15–22.

A. Ahmed-Zaïd, A. Moulla, M.S. Hantala and J.Y. Desmons, (2001), Amélioration des performances des capteurs solaires plans à air: application au séchage de l'oignon jaune et du hareng, *Revue des énergies renouvelables*, vol. 4, pp. 69-78.

A. Benkhelifa, (1998), Optimisation d'un Capteur Solaire Plan, *Revue des Energies Renouvelables : Physique Energétique*, pp. 13-18.

A. Labed, N. Moummi, K. Aoues and M. Zellouf, (2013), Etude expérimentale des performances thermiques et des pertes de charges de différentes configurations de capteurs solaires plans à air, In: 16ème Edition des *Journées Internationales de Thermique* (JITH2013).

A. Labed,N. Moummi, K. Aoues, M. Zellouf and A. Moummi, (2009), Etude théorique et expérimentale d'un capteur solaire plan à air muni d'une nouvelle forme de rugosité artificielle, *Revue des Energies Renouvelables*, Vol 12, pp. 551-561.

A.A. El-Sebaii, S. Aboul-Enein, M.R.I. Ramadan and E. El-Bialy, (2007), Year round performance of double pass solar air heater with packed bed, *Energy Conversion and Management*, Vol. 48, pp. 990–1003.

A.A. El-Sebaii, S. Aboul-Enein, M.R.I. Ramadan, S.M. Shalaby and B.M. Moharram, Thermal performance investigation of double pass-finned plate solar air heater, *Applied Energy*, Vol. 88, pp. 1727–1739.

A.E. Kabeel and K. Mečárik, (1998), Shape optimization for absorber plates of solar air collectors, *Renewable Energy*, Vol. 13, N°.1, pp. 121-131.

B. Djimasra, (2014), Contribution à l'étude du coefficient d'échange thermique dans un capteur solaire plan à dent de scie, Mémoire de Master, Ecole Nationale Supérieure des Sciences Agro-Industrielles de l'Université de Ngaoundéré, Cameroun.

D. Njomo, (1998), Étude théorique du comportement thermique d'un capteur solaire plan à air à couverture combinée plastique-vitre, *Revue Générale de Thermique,* Vol. 37, pp. 973-980.

D. Semmar, S. Betrouni and D. Lafri, (1998), Etude et Réalisation d'un Capteur Solaire à Air, *Revue des Energies Renouvelables : Physique Energétique*, pp.33-38.

F. A. Tetang, M. Edoun, X. Chesneau, A. Kuitche and B. Zeghmati, (2018), Modélisation du rendement thermique d'un insolateur double vitrage et double passe dans un environnement tropical humide, Fourth International Conference on Energy, Materials, Applied Energetics and Pollution, pp. 244-250.

K. Agbossou, F.A. Tetang, T.E. Boroze, K. N'wuitcha, K. Napo, B. Zeghmati, (2016), Theoretical and Experimental Study of Thermal Performance of Flat Plate Air Heating Collector, *International Journal of Science and Technology*, ISSN 2049-7318, Volume 5, N° 10, pp 473-490.

K. Aoues, N. Moummi, M. Zellouf and A. Benchabane, (2011), Thermal performance improvement of solar air flat plate collector: a theoretical analysis and an experimental study in Biskra, Algeria, *International Journal of Ambient Energy*, Vol. 32, No. 2, pp. 95–102.

M.A. Karim and M.N.A. Hawlader, (2006), Performance evaluation of a v-groove solar air collector for drying applications, *Applied Thermal Engineering*, Vol. 26, pp. 121–130.

M.W. Kareem, H. Khairul, K. Sopian and I. Kashif, (2016), Performance evaluation of a novel multi-pass solar air heating collector, *Procedia Engineering*, Vol. 148, pp. 638–645.

N. Moummi, S. Youcef-Ali, A. Moummi and J.Y. Desmons, (2004), Energy analysis of a solar air collector with rows of fins, *Renewable Energy*, Vol. 29, pp. 2053–2064.

R.R. Hwang, Y.C. Chow and Y.F. Peng, (1999), Numerical study of turbulent flow over-tow dimensional surface-mounted ribs in a channel, *International Journal for Numerical Methods in Fluids*, Vol. 37, pp. 767-785, 1999.

S. Bahria and M. Amirat, (2013), Influence de l'adjonction des chicanes longitudinales sur les performances d'un capteur solaire plan à air, *Revue des énergies renouvelables*, Vol. 16, pp. 51 – 63.

S. Oudjedi, A. Boubghal, W. Braham, T. Chergui and A. Belhamri, (2008), Etude paramétrique d'un capteur solaire plan à air destiné au séchage, *Revue des Energies Renouvelables*, pp. 255 – 266.

S. Youcef-Ali and J.Y. Desmons, (2006), Numerical and Experimental Study of a Solar Equipped with Offset Rectangular Plate Fin Absorber Plate, *Renewable Energy*, Vol. 31, N°13, pp. 2063–2075.

T. Beikircher, M. Möckl, P. Osgyan and G. Streib, (2015), Advanced solarflat plate collectors with full area absorber, front side film and rear side vacuum super insulation, *Solar Energy Materials & Solar Cells*, Vol. 141, pp. 398–406.

W. Gao, L. Wenxian and L. Enrong, (2000), Numerical study on natural convection inside the channel between the at-plate cover and sine-wave absorber of a cross-corrugated solar air heater, *Energy Conversion and Management*, Vol. 41, pp. 145-151.

Y. Jannot, (2011), Thermique solaire. 75 pages.